Wefer, G., Berger, W.H., and Richter, C. (Eds.)
Proceedings of the Ocean Drilling Program, Scientific Results Volume 175

18. Fluctuations in Productivity and Upwelling Intensity at Site 1083 during the Intensification of the Northern Hemisphere Glaciation (2.40–2.65 Ma)[1]

V.J. Ettwein,[2,3] C.E. Stickley,[2] M.A. Maslin,[2] E.R. Laurie,[2,3] A. Rosell-Melé,[4] L. Vidal,[5] and M. Brownless[6]

[1]Ettwein, V.J., Stickley, C.E., Maslin, M.A., Laurie, E.R., Rosell-Melé, A., Vidal, L., and Brownless, M., 2001. Fluctuations in productivity and upwelling intensity at Site 1083 during the intensification of the Northern Hemisphere glaciation (2.40–2.65 Ma). *In* Wefer, G., Berger, W.H., and Richter, C. (Eds.), *Proc. ODP, Sci. Results,*175, 1–25 [Online]. Available from World Wide Web: <http://www-odp.tamu.edu/publications/175_SR/VOLUME/CHAPTERS/SR175_18.PDF>. [Cited YYYY-MM-DD]
[2]Environmental Change Research Centre, Department of Geography, University College London, 26 Bedford Way, London WC1H 0AP, United Kingdom. Correspondence author: **v.ettwein@ucl.ac.uk**
[3]Centre for Quaternary Research, Department of Geography, Royal Holloway, University of London, Egham, Surrey TW20 0EX, United Kingdom.
[4]Quaternary Environmental Change Research Group, Department of Geography, University of Durham, Science Site, South Road, Durham DH1 3LE, United Kingdom.
[5]Universität Bremen, Geowissenschaften, Postfach 330440, D-28334 Bremen, Federal Republic of Germany. Present address: CEREGE, Université Aix-Marseille III, Europole de l'Arbois, BP 80, 13545 Aix en Provence, Cedex 04, France.
[6]Department of Geology, Royal Holloway, University of London, Egham, Surrey TW20 0EX, United Kingdom.

Initial receipt: 22 February 2000
Acceptance: 4 June 2001
Web publication: 10 August 2001
Ms 175SR-227

ABSTRACT

Coastal upwelling regions play an important role in regulating the partial pressure of CO_2, because they are zones of intense productivity and therefore contribute considerably to the drawdown mechanism. One of the major aims of Leg 175 was to develop an understanding of the relationship between wind-driven upwelling intensity and surface water productivity. In this paper, such a relationship during the late Pliocene intensification of the Northern Hemisphere glaciation (INHG) ~2.54 Ma is examined. Surface water productivity is reconstructed using principally diatoms and $\delta^{15}N$, but total organic carbon is also used to a lesser extent. Results are compared with "hard" isothermal remnant magnetism, a proxy for wind strength. Lying offshore on the Walvis Ridge, Site 1083 is ideally located for such a study as it is influenced by the center of the Benguela Current upwelling system and is distant from terrestrial sources which may affect the productivity signal. Prior to the INHG, strong frontal systems were found to be operative over the site, with little interglacial–glacial fluctuation in wind intensity and productivity. Following the INHG, the development of trade winds induced the formation of an upwelling regime. However, where wind intensity remained elevated throughout the succeeding glacial periods, productivity levels peaked sharply during the interglacial–glacial transi-

tions before falling again to levels comparable to those of interglacials. Such peaks during the initial stages of the glaciations may provide an important feedback mechanism for the further rapid, intensified cooling of global climate. $\delta^{15}N$ reconstructions of nutrient utilization, and the abundance of southern-source diatoms transported to the site via the nutrient-bearing Antarctic Intermediate Waters, suggest that productivity may have responded instead to the nutrient content of upwelled waters.

INTRODUCTION

The carbon reservoir within the oceans is 60 times greater than that of the atmosphere (e.g., Berger et al., 1989). A small change in the oceanic reservoir may strongly affect the atmospheric reservoir with which it exchanges. Perhaps the most important way in which the ocean can alter its ability to hold CO_2 is through changes in surface water productivity (Broecker, 1982). Such changes set the partial pressure of CO_2 (pCO_2) through both "biological pumping" (in which carbon is removed from surface waters to deep waters), and "biological dumping" (in which organic carbon is removed from the system through sedimentary deposition and burial) (Shipboard Scientific Party, 1998a). Coastal upwelling regions play an important role in this system because nutrient-rich waters, when vertically advected to the surface through the combined actions of wind forcing and Ekman pumping, induce intense surface water productivity. This acts as a huge sink for atmospheric CO_2.

The defining feature of the Quaternary era was the rapid expansion of the Northern Hemisphere ice sheets. This marked a unique period in climate history, when the planet entered into a state of bipolar glaciation. Numerous Ocean Drilling Program (ODP) records taken from the Northern Hemisphere suggest the intensification of Northern Hemisphere glaciation (INHG) took place in three stages at ~2.74, ~2.70, and ~2.54 Ma (reviewed in Maslin et al., 1998). However, the latter step associated with the expansion of the Laurentide Ice Sheet (i.e., the glaciation of northeast America) had the greatest effect on the global system (e.g., Maslin et al., 1998; Shackleton et al., 1995, 1984; Tiedemann et al., 1994). It has been suggested that the INHG occurred as a consequence of tectonically induced long-term cooling and was initiated by changes in orbital forcing (Haug and Tiedemann, 1998; Maslin et al., 1998), however the feedback mechanisms that translated this forcing into global climate change have still to be understood.

Northern Hemisphere glaciation would have altered atmospheric circulation patterns, and therefore wind-driven upwelling regimes, such as the Benguela Current (BC) upwelling system, which is among the five or six major upwelling regions of the world (Berger et al., 1998). Intermediate in intensity between the systems off Peru and California (Lange et al., 1999; Berger et al., 1998), it is located in the subtropical eastern South Atlantic, off the coast of Namibia, southeast Africa, extending from Cape Point (34°S) in the south to Cabo Frio (18°S) in the north (Lange et al., 1999), as shown in Figure **F1.**

The Benguela system is important because it incorporates the BC, a major surface water vector of heat and salinity toward the Brazilian Coastal Current (BCC) that crosses the equator. Consequently, it has a major influence on the cross-meridional flow of heat energy that influences global climate. Moreover, the BC system is also a major sink for

F1. Location of Site 1083, Leg 175, p. 21.

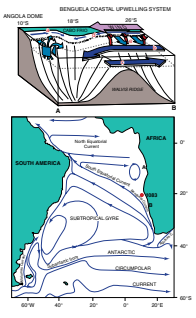

atmospheric CO_2. Both of these processes may be important climate feedbacks that contributed to the INHG.

Modern Hydrography

The modern oceanography of the region consists of a number of surface and deep-water currents and is shown in both aerial and schematic view in Figure F1. The BC is a shallow (<80 m), cool, surface water current flowing toward the Equator. It forms part of the eastern limb of the South Atlantic Gyre (Dowsett and Willard, 1996). The water of the BC is thought to originate from three sources (Garzoli and Gordon, 1996, and references therein): the South Atlantic Current (the southern limb of the South Atlantic subtropical gyre); the Agulhas Current (the warm south Indian Ocean western boundary current), and subantarctic water from the Antarctic Circumpolar Current (Antarctic Intermediate Water, AAIW).

Between 23° and 28°S (varying with the season), the BC splits into two components (Lange et al., 1999; Berger et al., 1998): the BCC, which transports cold, nutrient-rich water from the wind-dominated coastal area northward along the shelf (Schneider et al., 1997), and the Benguela Oceanic Current (BOC), which takes warmer water northwest by geostrophic flow (Holmes et al., 1996). The BCC is the weaker branch of the divergence (Hay and Brock, 1992), whereas the BOC is the stronger vector and transfers heat toward the Brazilian Coastal Current, and thus to the Northern Hemisphere (Berger et al., 1998). This, therefore, has important implications for global climate.

At ~16°S (Cabo Frio), the cold, northward-flowing BCC meets with the warm tropical/equatorial southward-flowing waters of the Angola Current (AC). This marks the position of the Angola Benguela Front (ABF), across which there is a sharp temperature gradient of 7.5°C (Holmes et al., 1996). At this point, the BCC subducts beneath the AC and continues northward into the Angola Basin as a shallow subsurface current (Holmes et al., 1997). The location of the ABF shifts between ~15°S during austral spring and ~17°S in austral autumn (Holmes et al., 1996).

Beneath the BCC is a poorly oxygenated poleward-flowing undercurrent (PUC), which is restricted to the edge of the shelf and upper slope, and centered at ~200–300 m depth (Berger et al., 1998, and references therein). It forms the eastern side of a cyclonic subsurface gyre that upwells the more oxygenated, nutrient-rich AAIW immediately beneath the pycnocline (Hay and Brock, 1992). Ventilation by the AAIW is considered to be directly proportional to the strength of the BC (Berger et al., 1998).

South of 15°S Ekman motion combined with south and southeast zonal trade winds from the African continent, cause waters to be upwelled over the inner shelf and shelf break (Holmes et al., 1997). This takes place within a narrow band not more than 100 km wide, mostly within the 300 m isobath (Hay and Brock, 1992). Although occurring as a year-round phenomenon in this region (Lalli and Parsons, 1997), upwelling is subject to variation resulting from the seasonal north-south migrations of the trade winds. During austral winter, the Intertropical Convergence Zone (ITCZ) shifts northward, pulling the subtropical high-pressure zone toward the equator (Diester-Haass et al., 1992). As a result, modern upwelling in the Benguela system is at its maximum during austral spring from December to April (Hay and Brock, 1992).

Upwelling varies alongshore in eight cells (Fennel, 1999), extending from 15° to 35°S, with the strongest signal found at Lüderitz, Namibia (27°S) (Lange et al., 1999).

Estimates of the depth from which waters are upwelled range from 150 m (Holmes et al., 1998) to 330 m (Hay and Brock, 1992). The depth of the pycnocline off Walvis Bay is considered to be only 250 m below the surface (Hay and Brock, 1992), enabling cold, nutrient-rich waters (from within the PUC) to be vertically advected into the photic zone. This results in high nearshore nutrient concentrations (Holmes et al., 1996) with coastal surface water nitrate and phosphate levels frequently reaching 30 and 2.5–8 µM/L, respectively (Holmes et al., 1998). Consequently, productivity levels are high, with carbon fixation rates reaching 125–180 g C/m² per yr (Berger, 1989; Holmes et al., 1996).

Site Description

The BC system was previously drilled by the Deep Sea Drilling Project (DSDP) (Legs 40, 74, and 75); however, most of these sites were considered too far offshore to provide a direct record of upwelling (Berger et al., 1998). Instead, they were interpreted to contain records of productivity from eddies that had been transported westward by the BC (Diester-Haass et al., 1992). Additionally, the cores were rotary drilled and considered too disturbed to permit high-resolution reconstructions (Berger et al., 1998). Nevertheless, a fairly detailed study of productivity was completed by Dowsett and Willard (1996) using sediments drilled from DSDP Site 532.

Sediments used in this study were taken from Site 1083 (20°53.6481′S, 11°13.0720′E), drilled during ODP Leg 175 during the summer of 1997. Site 1083 is situated near to the edge of the continental shelf and, together with Sites 1081 and 1082, and DSDP Sites 532 and 362, forms a rough north-south transect within the Walvis Ridge/Walvis Basin area. Four holes were drilled at the site, and sediments from Hole 1083A were used in this study.

Lying close to the major upwelling centers off southwest Africa, which at present maintain a year-round activity, these sites should directly record paleointensity fluctuations in coastal upwelling. Site 1083 is located the farthest from the shore, and is therefore expected to have the best representation of pelagic signals. It was also the deepest, drilled in a water depth of 2178 m (Berger et al., 1998). The lithology of the site throughout the time period investigated consisted of one single unit composed of moderately bioturbated clayey nannofossil ooze (Shipboard Scientific Party, 1998b).

Aim and Focus

This study attempts to reconstruct productivity within the BC upwelling system during the time of the expansion of the Laurentide Ice Sheet in the Northern Hemisphere, at ~2.54 Ma (Maslin et al., 1998, and references therein), principally using diatoms and nitrogen isotopes ($\delta^{15}N$). However total organic carbon (TOC) is also used to strengthen the interpretation. The relationship between productivity and upwelling is investigated through the "hard" isothermal remnant magnetism (HIRM) record, which serves as a proxy for wind strength, obtained from the same sediment.

Attention is focused on the time frame 2.40–2.65 Ma, not only to investigate the period of rapid ice-volume expansion but also to recon-

struct activity both prior to and immediately following the event. The reconstruction of a high-resolution record is achieved through a sampling interval of 20 cm (~2 k.y.). This will permit inferences to be made concerning the relationship between the Northern and Southern Hemispheres at times of ice-volume expansion.

TECHNIQUES AND METHODOLOGY

Diatoms

Diatoms are microscopic, unicellular, golden-brown algae belonging to the plant class Bacillariophyceae of the division Chromophyta (e.g., Hasle and Syvertsen, 1996). They are characterized by an external frustule (skeleton), typically 10–100 µm in length or diameter. This frustule is composed of amorphous silica (opal-A), which has the potential to be preserved within the sedimentary record.

Diatoms are ubiquitous to aquatic environments and as such are found in a wide range of habitats from terrestrial through brackish to fully marine. They are ecologically and environmentally sensitive and in the oceans constitute a major part of the marine phytoplankton.

Discrete samples were prepared for diatom analysis following a procedure modified from Battarbee (1986) for freshwater diatoms. Because of the high organic matter content, samples were left to stand in H_2O_2 overnight at room temperature before being gently heated in a water bath. Following the procedure of Battarbee and Kneen (1982), samples were spiked with a calibrated microsphere solution to enable quantitative data analysis. Diatom valves, including those of *Chaetoceros* resting spores, and microspheres were counted under a 400× phase objective lens with an Olympus BH-2 microscope. At least 300 valves were counted per slide.

All absolute abundance data were then converted to diatom accumulation rates (DARs) (e.g., Schuette and Schrader, 1979), to account for sedimentation rate (SR) and dry bulk density. Based upon the age model, the SR at Site 1083 over the investigated 250 k.y. ranged from 5.65 cm^2/k.y. (at 2.468–2.464 Ma) to 12.45 cm^2/k.y. (at 2.604–2.603 Ma), averaging at 9.45 cm^2/k.y. Formulas are given in "Appendix," p. 20.

Nitrogen Isotopes

Modern studies have shown oceanic productivity to be a function of nutrient availability, with nitrogen (principally in the form of nitrate [NO_3^-]) constituting one of the main limiting factors. Nitrogen limitation can have important implications for the amount of CO_2 drawdown within a system, for reasons related to the Redfield ratio. This states that during photosynthesis carbon, nitrogen, and phosphorus are taken up in the ratio 106:16:1 (Brasier, 1995). If NO_3^- is limiting within the system, there will be a net reduction in CO_2 drawdown, which creates a negative feedback within the system.

When NO_3^- is abundant, phytoplankton selectively discriminate against the isotopically heavier ^{15}N during photosynthetic uptake, preferring the isotopically lighter isotope ^{14}N. When NO_3^- is limited no discrimination is made (Ostrom et al., 1997). Organic matter should therefore yield a relatively lighter $\delta^{15}N$ (less positive) isotopic signature at

times when NO_3^- is in ready supply, and a relatively heavier (more positive) signal at times when NO_3^- supplies are limiting.

Marine studies (e.g., Holmes et al., 1996, 1997; Farrell et al., 1995; Francoise et al., 1993) have also identified this signal in the surface sediments. A relationship exists between the sedimentary $^{14}N/^{15}N$ ratio and NO_3^- utilization in the surface waters. If this relationship is extended downcore, past changes in the nutrient supply demand, balance can be hindcasted from records of $\delta^{15}N$ in organic matter (Holmes et al., 1996; Farrell et al., 1995). This technique has been used successfully to reconstruct paleo-NO_3^- utilization in the Gulf of California (e.g., Pride et al., 1999), in the southwest Indian sector of subantarctic waters (e.g., Francoise et al., 1993), and in the late Quaternary sediments off Angola (e.g., Holmes et al., 1996, 1997, 1998).

In addition, the $\delta^{15}N$ signal is sensitive to NO_3^- source (i.e., marine or terrestrial in origin). Analysis of the $\delta^{13}C$ signature in sedimentary organic matter can help identify the source. Marine algae utilize dissolved bicarbonate (HCO_3^-) for photosynthesis, yielding stable organic carbon isotope ratios of an average of –21‰ (Meyers, 1992). Land plants derive their carbon from atmospheric CO_2, which is isotopically lighter than marine HCO_3^-. Terrestrial organic matter typically has a $\delta^{13}C_{org}$ signature of about –28‰. Studies from DSDP Sites 362 and 532 suggest that the distinction between terrestrial and marine organic matter is well preserved in the sediments of the Walvis Ridge back to 14 Ma (Meyers, 1992).

Nitrogen isotope analysis was conducted on the raw sediment. For carbon isotope analysis, each sample was pretreated with HCl to remove the inorganic carbonate fraction. Analysis was conducted at the NERC Inductively Coupled Plasma–Atomic Emission Spectrometry (ICP-AES) facility at Royal Holloway, University of London, United Kingdom. Nitrogen and carbon isotopes are expressed in the standard delta notation as parts per thousand (‰), relative to atmospheric nitrogen, and Peedee belemnite standards, respectively. Error ranges were derived through replication of laboratory standards.

Total Organic Carbon Reconstruction

Details of this technique and the standard methodology employed are given in Rosell-Melé et al. (submitted, this volume [N1]), and Durham et al. (**Chap. 23,** this volume) (see also Rosell-Melé et al., 1997; Harris et al., 1996). TOC data were converted into mass accumulation rates (MAR) to account for the sedimentation rate and to enable more direct comparison with the diatom data.

AGE MODEL

The age model is derived from comparison of the $\delta^{18}O$ stratigraphy (*Cibicidoides wuellerstorfi*) with that of the reference record from ODP Site 607 (Raymo et al., 1992, updated by Bickert et al., 1997) (see Vidal et al., submitted, this volume [N2]). Glacial/interglacial periods (on Fig. F2 as gray/white bands, respectively) were derived from the midpoint between peaks and troughs in $\delta^{18}O$ following the procedure of Tiedemann et al. (1994) and provide the basis for interpretation in this study. The $\delta^{18}O$ curve indicates a significant trend toward glacial conditions at ~2.54 Ma. This corresponds to the INHG and associated increase in ice

F2. Downcore reconstructions vs. age for $\delta^{18}O$ vs. PDB, total organic carbon, *Chaetoceros* resting spores, Southern Ocean diatoms, and $\delta^{15}N$ vs. air, p. 22.

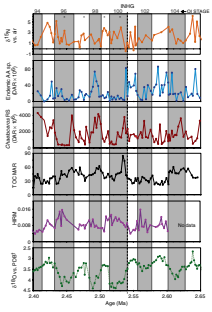

sheet volume in North America (e.g., by Maslin et al., 1995; 1998; Shackleton et al., 1984; 1995; Tiedemann et al., 1994).

RESULTS

Diatoms

Data for species common to the Antarctic and Subantarctic (e.g., Akiba, 1982; Johansen and Fryxell, 1985; Priddle and Fryxell, 1985; Fryxell et al., 1986; Baldauf and Barron, 1991; Fenner, 1991; Harwood and Maruyama, 1992; Hasle and Syvertsen, 1996) were combined to form an "Antarctic" (AA) group, representing diatoms transported from the Southern Ocean. The group comprises *Asteromphalus hookeri, Asteromphalus parvulus, Azpeitia tabularis, Dactyliosolen antarcticus, Fragilariopsis kerguelensis, Proboscia barboi, Rhizosolenia praebergonii, Thalassiosira poroseriata,* and *Thalassiothrix antarctica*. Of these, *T. antarctica* and *P. barboi* are the most abundant constituents of the AA group. Diatoms of the AA group were likely to have been living in Antarctic and Subantarctic open ocean waters. Those near the Antarctic polar frontal zone (APFZ) were likely to have been incorporated into the AAIW mass during its formation at this ocean front. Previous studies (e.g., Treppke et al., 1996) have also shown that displaced Southern Ocean diatoms present in the waters over the Walvis Ridge are transported within the AAIW. This watermass also serves as an important source of nutrients (Lange et al., 1999; Berger et al., 1998). Fluctuations in this group should, therefore, represent variation in the oceanography of the region, although changes in the productivity biomass cannot be ruled out. The DAR data for *Chaetoceros* resting spores and the AA group are shown in Figure **F2.**

The diatom assemblages at Site 1083 are dominated by *Chaetoceros* resting spores. Resting spore formation is associated with nutrient exhaustion in the water column, after mass multiplication of vegetative cells following an upwelling event (e.g., Bao et al., 1997, and references therein), often in highly-stratified waters (S. Boharty, pers. comm., 2001). *Chaetoceros* resting spores, therefore, provide a record of paleobloom events. Such qualities have led to their exploitation to great effect in many studies of both modern and paleo-upwelling regimes including southern Spain (e.g., Bárcena and Abrantes, 1998); northwest Iberia (e.g., Bao et al., 1997); California (e.g., Grimm et al., 1996; Hutchins and Bruland, 1998); Peru (e.g., Schrader and Sorknes, 1997), and the Antarctic region (e.g., Leventer, 1991; Rathburn et al., 1997). They have also been used in previous studies of the BC system (e.g., Treppke et al., 1996; Lange et al., 1999). Therefore, assuming that the abundance of *Chaetoceros* resting spores does not fluctuate in response to the changing intensity of biogenic silica dissolution, this proxy can be used with confidence to reconstruct productivity at Site 1083.

Chaetoceros resting spores comprise 33%–99% of the assemblage (averaging 76%), indicating that upwelling has been an important feature at this site throughout the whole of the time period investigated. This is in agreement with Lange et al. (1999), who reported their occurrence at Sites 1081, 1082, 1084, and 1085 in highly variable abundance throughout the same time period.

Prior to ~2.54 Ma, *Chaetoceros* resting spore abundance displays high sample-to-sample variability. Peaks in DAR occur with a periodicity of ~9–11 k.y. and maximum amplitude of ~4000 × 10^6 valves/cm^2 per k.y.

Maximum peaks in productivity occur during glacial Stages 104 (~3630 × 10^6 valves/cm^2 per k.y. at ~2.62 Ma) and 102 (~3320 × 10^6 valves/cm^2 per k.y. at ~2.57 Ma). Peaks of comparable magnitude also occur within interglacial Stages 105 (~3330 × 10^6 valves/cm^2 per k.y. at ~2.649 Ma) and 103 (~2890 × 10^6 valves cm^2 per k.y. at ~2.590 Ma). However, the latter peak is isolated so should be treated with caution. The data suggest overall that productivity was not significantly related to glacial/interglacial cyclicity at this time.

The DAR of the AA group is considerably higher and more variable between 2.65 and 2.54 Ma than the period following the INHG. Two sharp peaks in the DAR of the AA group correspond to those of *Chaetoceros* resting spores occurring at ~2.599 (~70 × 10^6 valves/cm^2 per k.y.) and ~2.558 Ma (~55 × 10^6 valves/cm^2 per k.y.).

After ~2.54 Ma, there appears to be a far more organized cyclicity within the *Chaetoceros* resting spores data. Peaks in the accumulation rate show an apparent cyclicity of ~30–35 k.y. Both the highest and lowest DAR values are found within this period during Stages 94 (~4250 × 10^6 valves/cm^2 per k.y. at ~2.406 Ma) and 96 (~320 × 10^6 valves/cm^2 per k.y. at ~2.447 Ma). As a consequence, the amplitude of the signal is much greater (an average of ~6400 × 10^6 valves/cm^2 per k.y.). Other peaks of significantly elevated *Chaetoceros* resting spore productivity occur during glacial Stages 100 (~3800 × 10^6 valves/cm^2 per k.y. at ~2.536 Ma), 98 (~4150 × 10^6 valves/cm^2 per k.y. at ~2.497 Ma and ~3700 × 10^6 valves/cm^2 per k.y. at ~2.492 Ma), and 96 (~4000 × 10^6 valves/cm^2 per k.y. at ~2.457 Ma) and during the interglacial Stage 95 (~3395 × 10^6 valves/cm^2 per k.y. at ~2.430 Ma). Peaks and troughs also appear to be more temporally sustained (i.e., a longer wavelength) where each oscillation encompasses a greater number of samples. This is especially so for the troughs found within the glacial Stages 100 and 96. Such temporal variability in DARs appears also to be a feature of the AA group, though on a comparatively lesser magnitude of scale.

The AA group DAR signal is suppressed following the INHG, but three prominent peaks occur at ~2.538 Ma (~80 × 10^6 valves/cm^2 per k.y.), ~2.492 Ma (~75 × 10^6 valves/cm^2 per k.y.), and ~2.428 Ma (~50 × 10^6 valves/cm^2 per k.y.). The former two occur within glacial Stages 100 and 98, respectively, and the latter corresponds to a similar peak in *Chaetoceros* resting spores within interglacial Stage 95.

After ~2.54 Ma the major peaks in *Chaetoceros* resting spores occur at the interglacial–glacial transitions (i.e., during ice accumulation). DAR peaks rise and fall sharply across the boundaries. Such peaks tend to correspond with similar fluctuations in the AA group, suggestive of a relationship between the two.

Stable Isotopes

Analysis of replicate laboratory standards produced error ranges of ± 0.2‰ and ± 0.1‰ for $\delta^{15}N$ an $\delta^{13}C_{org}$, respectively. Preliminary investigations of $\delta^{13}C_{org}$ values for Site 1083 (not shown here) range between –20.17‰ and –22.58‰, and average at –21.35‰ ± 0.1‰. This value indicates that the main source for the organic matter at Site 1083 is from marine algal production. This is in agreement with previous studies (e.g., by Treppke et al., 1996) that have shown the study area not to have been affected by input from the Cunene River. Therefore, the $\delta^{15}N$ signature of sediments from Site 1083 has the potential to contain a record of the nutrient utilization within the marine environment.

Where fluctuations in the $\delta^{13}C_{org}$ record should show changing productivity, this is related to the entire biological assemblage composing the organic matter. Fractionation may, therefore, be affected by changes within the entire biological assemblage of the site, and not necessarily reflect diatom abundance alone. For this reason, the $\delta^{13}C_{org}$ record is not discussed in detail here (see Maslin et al., unpubl. data).

The $\delta^{15}N$ values range between 6.11‰ and –0.45‰, and average 2.11‰ ± 0.2‰. The record shown in Figure F2 indicates great variability throughout the time period, but the overall relationship between $\delta^{15}N$ and *Chaetoceros* resting spores suggests NO_3^- limitation at times of low production. This is as expected since *Chaetoceros* resting spore formation is known to be sensitive to low NO_3^- conditions (e.g., Schuette and Schrader, 1979).

NO_3^- appears to have been at its least limiting during late Stage 101 and at the beginning of Stage 100 and most limiting during Stages 105 and 95. The difference between glacials and interglacials is not marked. However, there is an indication of reduced nitrate limitation during the interglacial–glacial transition periods following ~2.54 Ma.

This model of NO_3^- utilization remains tentative, however, because it assumes that the $\delta^{15}N$ signal is a reflection of NO_3^- utilization within the water column. In reality, the signal may be recording a response to a wide variety of factors, reflecting the complexity of the nitrogen cycle.

Fractionation of the isotopes may occur at any point within the cycle and both before and after assimilation by phytoplankton, therefore affecting the isotopic ratio in the environment. Key areas of alteration are highlighted in Table T1.

T1. Potential sources of alteration in the $\delta^{15}N$ signal, p. 24.

Of the potential sources of alteration, only terrigeneous input can be disregarded with confidence, because $\delta^{13}C$ results indicate that the sedimentary organic matter is marine in origin at Site 1083. However, in previous studies of the Benguela system (e.g., Holmes et al., 1998, 1997, 1996), only diagenesis and denitrification are consistently considered to affect the $\delta^{15}N$ record.

At present, the effects of diagenesis are poorly understood. For the Southern Ocean, Altabet and Francoise (1994) report $\delta^{15}N$ at the sediment/water interface was enriched by 5‰ to 9‰ compared to the surface waters. However, for the North Atlantic, Altabet et al. (1991) report a depletion of $\delta^{15}N$ with depth. Whereas the former is consistent with oxidative degradation of organic matter, the latter was attributed to a gain of ^{14}N or a loss of ^{15}N. Nevertheless, the majority of studies to date have shown that the $\delta^{15}N$ signal of the surface waters is transferred to the surface sediments, albeit with a constant offset. For the Walvis Ridge area, modern studies have shown this offset to be 1.6‰ (Holmes et al., 1998).

Denitrification, however, may be of importance, as it is likely to have some temporal variability. Most phytoplankton assemblages are dominated by cyanobacteria (Falkowski et al., 1998), so there is much potential for denitrification to take place, especially in zones of enhanced productivity. The modern Benguela system is known to be oxygen depleted, particularly near to the coast (Holmes et al., 1998). However, O_2 is generally 1–2 mL O_2/L, but denitrification takes place only when levels are <0.2 ml O_2/L. Although concentrations this low are rarely observed on the shelf, they may occur. Studies of the modern Benguela system by Estrada and Marrasé (1987) showed that in April 1986, a subsurface NO_3^- minima coincided with a nitrite maxima and an oxygen

minima, suggesting denitrification had taken place at 23°S. Boulégue and Denis (1983) also suggested that anoxia was responsible for both fish kills and enhanced sulfide production that have been observed on the shelf within the same area.

It is difficult to speculate on the effects of denitrification in this record. If such a process had taken place, it would manifest itself as a more positive excursion in $\delta^{15}N$. This may have occurred at periods within the record when correlation with productivity indicators is poor (shown by asterisks in Fig. F2). The present data, however, is insufficient to indicate this with any great certainty. Nevertheless, productivity is still taking place at these points, suggesting that denitrification was not sustained and intense.

Total Organic Carbon

Similarly for the *Chaetoceros* resting spore record, TOC fluctuates with low amplitude within each climatic state throughout the time period prior to ~2.54 Ma, although levels are more elevated throughout Stage 104 (see Fig. F2). The lowest recorded TOC MAR occurs within this time period at ~2.593 Ma (21.06 g/cm per k.y.).

After ~2.54 Ma, the signals increase to more elevated levels, with records peaking at the interglacial–glacial transitions. This is particularly true for Stages 100 (~2.534 Ma) and 98 (~2.497 Ma), where there is a strong accordance with the record for *Chaetoceros* resting spores. However, where the *Chaetoceros* resting spores signal falls sharply after the initial peak during Stage 96, TOC MAR remains elevated.

Berger et al. (1998) suggested that silica might have been limiting within the Benguela region within the later stages of the Pleistocene. Silica (in the form of silicic acid) is a major requirement for diatoms for the construction of the frustule during cell division (e.g., Schrader and Schuette, 1981). Its limitation is less likely to affect nonsiliceous primary producers and may go some way to explaining the elevated TOC and chlorine MAR signals with a reduction in diatom production for this period. Alternatively, frustule dissolution in the water column is more likely to have taken place when concentrations of dissolved silica are reduced. Therefore, biosiliceous preservational issues must also be considered in this case.

DISCUSSION

Paleoceanographic Interpretations of Productivity Data

Because oceanic water is undersaturated in silica, diatom frustules will start to dissolve following bacterial degradation of their organic coating (e.g., Barron, 1993). Consequently, the diatom fossil record is not likely to represent the totality of the surface-dwelling living assemblage (e.g, Barron and Baldauf, 1989; Barron, 1993), and therefore, their relationship is not direct (Schrader and Schuette, 1981). However, the abundance of planktonic marine diatoms in surface and core sediments is directly related to surface water productivity (e.g., Barron and Baldauf, 1989), where highly productive surface waters are able to sustain more diatom growth than poorly productive waters. For example, during bloom events, the abundance of diatoms in a given volume of seawater may increase one hundredfold (e.g., Barron, 1993). In these

situations, opal export production rates may exceed the rates of dissolution within the marine environment, thus permitting better representation of surface water productivity within the sediment (Schneider et al., 1997, and references therein). Indeed, previous studies of the upwelling areas (e.g., Bárcena and Abrantes, 1998; Treppke et al., 1996) have shown a close correspondence between the species found at the sediment/water interface and those found within the photic waters above.

The bulk of diatom dissolution takes place within the upper 1000 m of the water column ("silica corrosion zone"), and within the upper 1–2 cm of the sediment (e.g., Schrader and Schuette, 1981). Therefore for good preservation within the record (little breakage and abundant whole valves [e.g., Burckle and Cirilli, 1987]), both descent through the water column and the SR must be rapid. A high SR is recorded at Site 1083 (average 9.45 cm/k.y.). The descent through the water column for individual diatoms may be of the order of 100 yr (e.g., Burckle and Cirilli, 1987). Sinking is greatly facilitated through clumping via incorporation into zooplankton fecal pellets and/or marine snow, or through flocculation with other diatoms and clay particles. Descent within zooplankton fecal pellets has been measured at up to 30–400 m/day in the Southern Ocean (Burckle and Cirilli, 1987), which in addition may serve to limit degradation by enclosing diatoms within protective organic "capsules" (Lalli and Parsons, 1997).

Descent through flocculation can occur in *Chaetoceros* resting spores where an adhesive marine gel is secreted (Grimm et al., 1996) to stimulate clumping and rapid "self"-sedimentation. By possessing both a highly silicified (and therefore relatively dissolution-resistant) frustule-adopting and this self-sedimentation strategy, *Chaetoceros* resting spores have the potential to be well preserved within marine sediments.

From the data presented in this study, it is proposed that intense upwelling-driven productivity was not a significant feature of the time period prior to the INHG at ~2.54 Ma, with comparatively little fluctuation between interglacial and glacial periods. HIRM data from the same sediments, which can be used to infer wind intensity, also reveal little change in the atmospheric systems operative within the two climatic states strength (shown in Fig. F2 for comparison). This is consistent with the concept that the ITCZ was in a more northerly position at this time, and a strong trade wind system had not yet developed (Hay, 1993; Hay and Brock, 1992). Similar results were found from diatom studies at Site 1084, where the presence of diatom mats (not recorded at this site) were used to infer strong frontal systems in operation at this time (Berger et al., 1998). Although it would still have occurred, upwelling would have been weaker, a suggestion that is supported by $U^{k'}_{37}$ sea-surface temperature data (A. Rosell-Melé and M.A. Maslin, unpubl. data), which show sustained warmer temperatures, with little fluctuation. This record is considered to be reliable, as the $U^{k'}_{37}$ index is unaffected by passage through the food chain and diagenesis (Treppke et al., 1996). Consequently, it has been used very successfully in paleoclimatic studies of modern glacial/interglacial sediments (e.g., Rosell-Melé et al., 1997; Schneider et al., 1995; Kennedy and Brassell, 1992).

The data presented here would suggest that following the INHG a productivity regime with strong interglacial–glacial contrast developed. Previous studies have proposed the development and intensification of the trade winds about this time (e.g., Hay and Brock, 1992; Hay, 1993), where, as a result of ice accumulation up in the Northern Hemisphere, the ITCZ shifted southward, prompting alteration of the thermal gradi-

ent. This would have caused the longshore winds (brought about by the low-pressure cell over the Namib Desert) to intensify through the constraints created by the escarpment of the Kalahari Plateau, (Dowsett and Willard, 1996), thereby initiating development of a strong upwelling regime. Upwelling is therefore inferred to have intensified during the glacial periods (Stages 100, 98, 96, 94). This is supported by the $U^{k'}_{37}$ sea-surface temperature record (Rosell-Melé and Maslin, unpubl. data), whereby glacials correspond with marked cold periods that are attributed to the intensified upwelling of colder waters. In addition, the HIRM data suggest that in comparison to the interglacial periods, the wind intensity increased and remained pronounced throughout the glacials following the INHG. Such a model of the wind regime is illustrated in Figure **F3A.**

However, in the case for productivity, the three independent sets of data all suggest that there is an initial surge during the glaciation periods, after which levels fall to values similar to those of the previous interglacial stage. This is shown in Figure **F3B,** which charts the productivity signal chiefly derived from the record of *Chaetoceros* resting spores. Such a divorce between inferred wind strength (and therefore upwelling) and productivity would suggest that glacial productivity within the waters above Site 1083 was, in fact, not predominantly controlled by wind-driven upwelling but rather by some factor influencing productivity over Site 1083.

F3. Simplified summary of events prior to and succeeding the intensification of the Northern Hemisphere glaciation, p. 23.

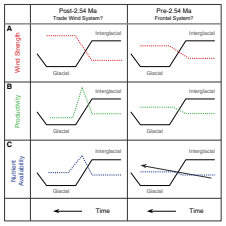

Control on Benguela Current Productivity

During upwelling, nutrient-rich waters are vertically advected from depths of 200–330 m, from within the poleward-flowing undercurrent (Dowsett and Willard, 1996). The nutrient pool of this water body is derived from the ventilation by the underlying AAIW (see **"Modern Hydrography,"** p. 3). Downhole variations in abundance of the AA diatom group reflect changes in the nature of the influence of AAIW (and thus its corresponding contribution to the nutrient pool) on upwelled waters. The diatom data show that during highly productive glaciation periods following the INHG there are often concomitant increases in the abundance of Southern Ocean species. This suggests changes in the nutrient regime of the system at these times.

Experimentation has shown that nitrogen deficiency is the single factor that consistently induces spore formation (Leventer, 1991, and references therein; Schuette and Schrader, 1979). Therefore, resting spore formation should take place as soon as NO_3^- becomes a limiting factor within the environment. Providing that there is representational preservation, the abundance of spores could potentially reflect the initial level of NO_3^- available within the system, with high abundances of *Chaetoceros* resting spores indicating periods when nutrients were in plentiful supply. Such enhanced supply could explain the periods of high productivity (reflected in all three productivity indicators) during the initial glaciations, and the corresponding lighter $\delta^{15}N$ values indicative of lesser nitrate limitation within the system at these times (Fig. **F3C**). This suggests that surface productivity is primarily controlled by the nutrient budget of the upwelled waters, rather than the rate of overturning.

Figure **F3** is a simplified summary interpretation of the wind strength-productivity-nutrient availability relationship, as revealed by data in this study, for the time periods both before and after the INHG.

Prior to ~2.54 Ma, a transition from interglacial to glacial conditions initiates a response within all three proxies in the same direction. However, following the INHG, the system response differs in that where the productivity and nutrient-content signals remain coupled, they are not necessarily linked with wind intensity (and therefore upwelling intensity).

The question arises, therefore, as to what is exerting a control over the concentration of the nutrient pool over the site. Upwelling of a more intense nature or the upwelling of more fertile waters, would both act to increase the supply of nutrients to the photic zone. In the first scenario, an increase in upwelling intensity would have the effect of increasing the rate at which nutrients were delivered to the surface waters, therefore increasing the concentration of the nutrient pool per unit time. This could be reflected by simultaneously elevated abundances in both the AA group (via the enhanced upwelling of AAIW-derived waters) and *Chaetoceros* resting spores (due to elevated productivity). In the second scenario, factors affecting the initial nutrient content of the upwelled waters per unit time (i.e., the fertility of the ventilating AAIW) must be addressed: AAIW forms to the south of the APFZ, where upwelled NADW mixes with Antarctic surface water. Because its density is greater than that of the water to the north, this water sinks to a depth of between 100 and 800 m (Dowsett and Willard, 1996). The extent of the Antarctic sea ice affects the fertility of the AAIW that is released to the wider oceans. For example, during the early Pliocene, the extent of sea ice was at a minimum, and the APFZ was displaced toward the Antarctic continent (Dowsett and Willard, 1996). This created a much larger surface water area within which planktonic oceanic Antarctic diatoms proliferated and depleted the water of nutrients. By the time this water was upwelled in the Benguela system, it would have been already depleted of nutrients (and relatively richer in AA diatoms), thus limiting surface water productivity at Site 1083. When the ice volume of the Antarctic continent expanded again, it created a narrowing of the diatom belt, leading to underutilization of the nutrients in the surface waters of the Southern Ocean. In this case, the AAIW reaching the BC would have been comparatively enriched in nutrients (and relatively depleted in AA diatoms) stimulating productivity at Site 1083. Therefore, the concentration of the nutrient pool per unit volume of water affected productivity in this case.

The fertility-related AA component of the diatom assemblage may therefore reflect either a change in upwelling intensity or a change of the concentration of AA diatoms within the same unit volume of upwelled water. Changes in productivity over Site 1083 can therefore reflect three scenarios:

- Where source fertility remains constant, productivity occurs as a response to a change in the intensity of upwelling (therefore, transporting more or less nutrients from the source into the photic zone, per unit time).
- Where upwelling intensity remains constant, productivity occurs as a response to a change in the nutrient content per unit volume of upwelled water (i.e., fertility).
- A combination of the above, whereby upwelling intensity and source fertility have both altered.

Although proxies indicative of wind intensity, productivity, AAIW influence, and mode of nutrient utilization are presented in this paper, it

is unlikely that such data can suggest to what extent the productivity is responding to each scenario. However the "combination" scenario seems most probable, because oceanographic and atmospheric systems are both known to alter in response to climate change.

Link between Productivity and Climate

Increases in primary production within the early glacials could have important implications for global climate, since they represent periods of enhanced CO_2 drawdown—a well-known feedback mechanism in the reduction of global temperatures. Because increased production is coeval with more rapid positive excursions in the $\delta^{18}O$ signal (especially during Stage 100), an important link exists between oceanic productivity and the decline to more pronounced glacial conditions following the INHG.

CONCLUSIONS

The following conclusions can be drawn from this work:

1. Prior to the INHG, the data are suggestive of strong frontal systems operative over Site 1083, with little interglacial–glacial contrast in the productivity signal.
2. Following the INHG, a wind-driven upwelling regime developed over Site 1083, which was more intense during glacial periods as reflected in the abundance changes in *Chaetoceros* resting spores. However such an upwelling regime is not reflected within the record of productivity, implying that productivity was not controlled by upwelling intensity. Productivity was instead controlled by the supply of nutrients to the photic zone from the AAIW, as suggested by the $\delta^{15}N$ record and the abundance of endemic Southern Ocean species within the diatom assemblage.
3. The nutrient budget of the photic zone may have been a reflection of a change in upwelling intensity where more nutrients were advected to the surface per unit time; or a change in the fertility of the AAIW, in which more nutrients were advected to the surface per unit volume of water. Although the actual mode of nutrient supply is undetermined from this study, it is likely to have been from a combination of these models.

Following the INHG, productivity levels surged to a peak at each interglacial–glacial transition. Such elevated levels of CO_2 drawdown could have provided an important feedback mechanism for the rapid decline into planetary glaciation.

It is not known whether the difference in the system holds for the time period prior to the that of this investigation. Therefore, additional investigation is required to further examine the possible relationship between oceanic productivity and climate before the intensification of the Northern Hemisphere glaciation at ~2.54 Ma.

ACKNOWLEDGMENTS

This work was conducted as an integral part of the master's of science degree in Quaternary Science, conducted jointly at Royal Holloway,

University of London, and University College London, and gratitude is extended to the Course Director, Rob Kemp. The authors are also grateful to the Ocean Drilling Program for providing material and to the Natural Environment Research Council for supporting this study (grant GST/02/2690, "The role of the Benguela Current upwelling system in controlling the intensification of Northern Hemisphere glaciation"). The authors would also like to acknowledge Carina Lange for valuable discussions concerning diatom taxonomy and Phil Meyers, Dyke Andreasen, and Marcus Kienast for great insight into the use of nitrogen isotopes. We thank Nick Branch, Janet Hope, and all members at the Centre for Quaternary Research (RHUL) and Environmental Change Research Centre (UCL) for technical assistance throughout this project; and Nick Mann and Catherine Pyke of the Department of Geography Drawing Office at UCL. The authors would also like to express their gratitude to Juliane Fenner and Steve Bohaty, who both provided valuable comments on an earlier version of this paper.

REFERENCES

Akiba, F., 1982. Late Quaternary diatom biostratigraphy of the Bellingshausen Sea, Antarctic Ocean. *Rep. Tech. Res. Cen. J.N.O.C.,* 16:31–74.

Altabet, M.A., and Francois, R., 1994. Sedimentary nitrogen isotopic ratio as a record for surface ocean nitrate utilization. *Global Biogeochem. Cycles,* 8:103–116.

Altabet, M.A., Deuser, W.G., Honjo, and S., Steinen, C., 1991. Seasonal and depth-related changes in the source of sinking particles in the North Atlantic. *Nature,* 6349:136–139.

Altabet, M.A., Francoise, R., Murray, D.W., and Prell, W.L., 1995. Climate-related variations in denitrification in the Arabian Sea from sediment $^{15}N/^{14}N$ ratios. *Nature,* 6514:506–509.

Baldauf, J.G., and Barron, J.A., 1991. Diatom biostratigraphy: Kerguelen Plateau and Prydz Bay regions of the Southern Ocean. *In* Barron, J., Larsen, B., et al., *Proc. ODP, Sci. Results,* 119: College Station, TX (Ocean Drilling Program), 547–598.

Bao, R., Varela, M., and Prego, R., 1997. Mesoscale distribution patterns in surface sediments as tracers of coastal upwelling of the Glacian shelf (NW Iberian Peninsula). *Mar. Geol.,* 144:117–130.

Bárcena, M.A., and Abrantes, F., 1998. Evidence of a high-productivity area off the coast of Málaga from studies of diatoms in surface sediments. *Mar. Micropaleon.,* 35:91–103.

Barron, J.A., 1993. Diatoms. *In* Lipps, J.E. (Ed.), *Fossil Prokaryotes and Protists:* Boston (Blackwell Scientific Pubs.), 155–167.

Barron, J.A., and Baldauf, J.G., 1989. Tertiary cooling steps and paleoproductivity as reflected by diatoms and biosiliceous sediments. *In* Berger, W.H., Smetacek, V.S., and Wefer, G. (Eds.), *Productivity of the Oceans: Present and Past:* New York (Wiley-Interscience), 341–354.

Battarbee, R.W., 1986. Diatom analysis. *In* Berglund, B.E. (Ed.), *Handbook of Holocene Paleoecology and Paleohydrology:* London (Wiley), 527–570.

Battarbee, R.W., and Kneen, M.J., 1982. The use of electronically counted microspheres in absolute diatom analysis. *Limnol. Oceanogr.,* 1:184–188.

Berger, W.H., 1989. Global maps of ocean productivity. *In* Berger, W.H., Smetacek, V.S., and Wefer, G. (Eds.), *Productivity of the Oceans: Present and Past:* New York (Wiley and Sons), 429–455.

Berger, W.H., Smetacek, V.S., and Wefer, G., 1989. Ocean productivity and paleoproductivity: an overview. *In* Berger, W.H., Smetacek, V.S., and Wefer, G. (Eds.), *Productivity of the Oceans: Present and Past:* New York (Wiley and Sons), 1–34.

Berger, W.H., Wefer, G., Richter, C., Lange, C.B., Giraudeau, J., Hermelin, O., and Shipboard Scientific Party, 1998. The Angola-Benguela upwelling system: paleoceanographic synthesis of shipboard results from Leg 175. *In* Wefer, G., Berger, W.H., and Richter, C., et al., *Proc. ODP, Init. Repts.,* 175: College Station, TX (Ocean Drilling Program), 505–531.

Bickert, T., Curry, W.B., and Wefer, G., 1997. Late Pliocene to Holocene (2.6–0 Ma) western equatorial Atlantic deep-water circulation: inferences from benthic stable isotopes. *In* Shackleton, N.J., Curry, W.B., Richter, C., and Bralower, T.J. (Eds.), *Proc. ODP, Sci. Results,* 154: College Station, TX (Ocean Drilling Program), 239–253.

Boulégue, J., and Denis, J., 1983. Sulfide speciations in upwelling areas. *In* Suess, E. and Theide, J., (Eds.), 1983. *Coastal Upwelling, Its sediment record. Part A: Responses of the Sedimentary Regime to Present Coastal Upwelling:* New York (Plenum Press and NATO Scientific Affairs Div.), 439–454.

Brasier, M.D., 1995. Fossil indicators of nutrient levels. 1: Eutrophication and climate change. *In* Bosence, D.W., and Allison, P.A. (Eds.), *Marine Palaeoenvironmental Analysis from Fossils.* Geol. Soc. Spec. Publ. London, 83:113–132.

Broecker, W.S., 1982. Ocean chemistry during glacial time. *Geochim. Cosmochim. Acta,* 46:1689–1705.

Bronk, D.A., and Ward, B.B., 1999. Gross and net nitrogen uptake and DON release in the euphotic zone of Monterey Bay, California. *Limnol. Oceanogr.,* 573–585.

Burckle, L.H., and Cirilli, J., 1987. Origin of diatom ooze belt in the Southern Ocean: implications for late Quaternary paleoceanography. *Micropaleontology,* 33:82–86.

Capone, D.G, and Carpenter, E.J., 1982. Nitrogen fixation in the marine environment. *Science,* 217:1140–1142.

Diester-Haass, L., Meyers, P.A., and Rothe, P., 1992. The Benguela Current and associated upwelling on the southwest African margin: a synthesis of the Neogene-Quaternary sedimentary record at DSDP Sites 362 and 352. *In* Summerhayes, C.P., Prell, W.L., and Emeis, K.C. (Eds.), *Upwelling Systems: Evolution Since the Early Miocene*. Geol. Soc. Spec. Publ. London, 64:331–342.

Dowsett, H., and Willard, D., 1996. Southeast Atlantic marine and terrestrial response to middle Pliocene climate change. *Mar. Micropaleontol.,* 27:181–193.

Estrada, M., and Marrasé, C., 1987. Phytoplankton biomass and productivity off the Namibian coast. *S. Afr. J. Mar. Sci.,* 5:347–356.

Falkowski, P.G., 1997. Evolution of the nitrogen cycle and its influence on the biological sequestration of CO_2 in the ocean. *Nature,* 387:273–275.

Falkowski, P.G., Barber, R.T., and Smetacek, V., 1998. Biogeochemical controls and feedbacks on ocean primary production. *Science,* 281:201–207.

Farrell, J.W., Pedersen, T.F., Calvert, S.E., and Nielsen, B., 1995. Glacial-interglacial changes in nutrient utilization in the equatorial Pacific Ocean. *Nature,* 377:515–517.

Fennel, W., 1999. Theory of the Benguela Upwelling System. *J. Phys. Oceanogr.,* 29:177–190.

Fenner, J.M., 1991. Late Pliocene-Quaternary quantitative diatom stratigraphy in the Atlantic sector of the Southern Ocean. *In* Ciesielski, P.F., Kristoffersen, Y., et al., *Proc. ODP, Sci. Results,* 114: College Station, TX (Ocean Drilling Program), 97–121.

Francoise, R., Bacon, M.P., and Altabet, M.A., 1993. Glacial/interglacial changes in sediment rain rate in the SW Indian sector of subantarctic waters as recorded by ^{230}Th, ^{231}Pa, U, and δ^{15}N. *Paleoceanography,* 8:611–629.

Fryxell, G.A., Sims, P.A., and Watkins, T.P., 1986. *Azpeitia* (Bacillariophyceae): related genera and promorphology. *Syst. Bot. Monogr.,* 13:1–74.

Ganeshram, R.S., Pedersen, T.F., Calvert, S.E., and Murray, J.W., 1995. Large changes in oceanic nutrient inventories from glacial to interglacial periods. *Nature,* 376: 755–758.

Garzoli, S.L., and Gordon, A.L., 1996. Origins and variability of the Benguela Current. *J. Geophys. Res.,* C1:897–906.

Grimm, K.A., Lange, C.B., and Gill, A.S., 1996. Biological forcing of hemipelagic sedimentary laminae: evidence from ODP Site 893, Santa Barbara Basin, California. *J. Sediment. Res.,* 66:613–624.

Harris, P.G., Zhao, M., Rosell-Melé, A., Tiedemann, R., Sarnthein, M., and Maxwell, J.R., 1996. Chlorine accumulation rate as a proxy for Quaternary marine primary productivity. *Nature,* 383:63–65.

Harwood, D.M., and Maruyama, T., 1992. Middle Eocene to Pleistocene diatom biostratigraphy of Southern Ocean sediments from the Kerguelen Plateau, Leg 120. *In* Wise, S.W., Jr., Schlich, R., et al., *Proc. ODP, Sci. Results,* 120: College Station, TX (Ocean Drilling Program), 683–733.

Hasle, G.R., and Syvertsen, E.E., 1996. Marine diatoms. *In* Tomas, C.R. (Ed.), *Identifying Marine Diatoms and Dinoflagellates:* New York (Academic Press), 5–386.

Haug, G.H., and Tiedemann, R., 1998. Effect of the formation of the Isthmus of Panama on Atlantic Ocean thermohaline circulation. *Nature,* 393:673–676.

Hay, W.W., 1993. Pliocene–Quaternary upwelling in the southeastern Atlantic may reflect changes in the water mass production, *Proc. 1st R.C.A.N.S. Cong. Lisbon* (*Ciências da Terra [UNL]*), 12:191–201.

Hay, W.W., and Brock, J.C., 1992. Temporal variation in intensity of upwelling off southwest Africa. *In* Summerhayes, C.P., Prell, W.L., and Emeis, K.C. (Eds.),

Upwelling Systems: Evolution Since the Early Miocene. Geol. Soc. Spec. Publ. London, 64:463–497.

Holmes, E.M., Muller, P.J., Schneider, R.R., Segl, M., Patzold, J., and Wefer, G., 1996. Stable nitrogen isotopes in Angola Basin surface sediments. *Mar. Geol.,* 134:1–12.

Holmes, M.E., Muller, P.J., Schneider, R.R., Segl, M., and Wefer, G., 1998. Spatial variations in euphotic zone nitrate utilization based on $\delta^{15}N$ in surface sediments. *Geo-Mar. Lett.,* 18:58–65.

Holmes, M.E., Schneider, R.R., Muller, P.J., Segl, M., and Wefer, G., 1997. Reconstruction of past nutrient utilization in the eastern Angola Basin based on sedimentary $^{14}N/^{15}N$ ratios. *Paleoceanography,* 4:604–614.

Hutchins, D.A., and Bruland, K.W., 1998. Iron-limited diatom growth and Si:N uptake ratios in a coastal upwelling regime. *Nature,* 393:561–564.

Johansen, J.R., and Fryxell, G.A., 1985. The genus *Thalassiosira* (Bacillariophyceae): studies on species occurring south of the Antarctic Convergence Zone. *Phycologia,* 24:155–179.

Karl, D., Letelier, R., Tupas, L., Dore, J., Christian, J., and Hebel, D., 1997. The role of nitrogen fixation in biogeochemical cycling in the subtropical North Pacific Ocean. *Nature,* 388:533–539.

Kennedy, J.A., and Brassell, S.C., 1992. Molecular records of twentieth century El-Niño events in laminated sediments from the Santa Barbara basin. *Nature,* 357:62–64.

Lalli, C.M., and Parsons, T.R., 1997. *Biological Oceanography, an Introduction,* Open Univ.: Oxford (Butterworth Heinemann).

Lange, C.B, Berger, W.H., Lin, H.-L., Wefer, G., and Shipboard Scientific Party, 1999. The early Matuyama diatom maximum off SW Africa, Benguela Current System (ODP Leg 175). *Mar. Geol.,* 161:93–114.

Leventer, A., 1991. Sediment trap diatom assemblages from the northern Antarctic Peninsula region. *Deep-Sea Res.,* 8/9:1127–1143.

Maslin, M.A., Haug, G.H., Sarnthein, M., and Tiedemann, R., 1995. The progressive intensification of the northern hemisphere glaciation as seen from the North Pacific. *Geol. Rundsch.,* 85:452–465.

Maslin, M.A., Li, X.S., Loutre, M-F., and Berger, A., 1998. The contribution of orbital forcing to the progressive intensification of Northern Hemisphere glaciation. *Quat. Sci. Rev.,* 17:411–426.

Meyers, P.A., 1992. Organic matter variations in sediments from DSDP Sites 362 and 532: evidence of upwelling changes in the Benguela Current upwelling system. *In* Summerhayes, C.P., Prell, W.L., and Emeis, K.C. (Eds.), *Upwelling Systems: Evolution Since the Early Miocene*. Geol. Soc. Spec. Publ. London, 64:323–329.

Naqvi, S.W.A., Yoshinari, T., Brandes, J.A., Devol, A.H., Jayakumar, D.A., Narvekar, P.V., Altabet, M.A., and Codispoti, L.A., 1998. Nitrogen isotopic studies in the suboxic Arabian Sea. *Proc. Ind. Acad. Sci.-Ear. Plan. Sci.,* 4:367–378.

Ostrom, N.E., Macko, S.A., Deible, D., and Thompson, R.J., 1997. Seasonal variation in the carbon and nitrogen isotope biogeochemistry of a coastal cold ocean environment. *Geochim. Cosmochim. Acta,* 14:2929–2942.

Peters, K.E., Sweeney, R.E., and Kaplan, I.R., 1978. Correlation of carbon and nitrogen stable isotope ratios in sedimentary organic matter. *Limnol. Oceanogr.,* 23:598–604.

Priddle, J., and Fryxell, G.A., 1985. *Handbook of the Common Plankton Diatoms of the Southern Ocean: Centrales Except the Genus Thalassiosira:* Cambridge (Cambridge Univ. Press).

Pride, C., Thunell, R., Sigman, D., Keigwin, L., and Altabet, M.A., 1999. Nitrogen isotopic variations in the Gulf of California since the last deglaciation: response to global climatic change. *Paleoceanography,* 3:397–409.

Rathburn, A.E., Pichon, J-J., Ayress, M.A., and De Deckker, P., 1997. Microfossil and stable-isotope evidence for changes in the late Holocene paleoproductivity and paleoceanographic conditions in the Prydz Bay region of Antarctica. *Paleogeogr., Paleoclimatol., Paleoecol.,* 131: 485–510.

Raymo, M.E., Hodell, D., and Jansen, E., 1992. Response of deep ocean circulation to initiation of Northern Hemisphere glaciation (3–2 Ma). *Paleoceanography,* 7:645–672.

Rosell-Melé, A., Maslin, M.A., Maxwell, J.R., and Schaeffer, P., 1997. Biomarker evidence for "Heinrich" events. *Geochim. Cosmochim. Acta,* 61:1671–1678.

Schneider, R.R., Müller, P.J., and Ruhland, G., 1995. Late Quaternary surface circulation in the east equatorial South Atlantic: evidence from alkenone sea surface temperatures. *Paleoceanography,* 10:197–219.

Schneider, R.R., Price, B., Müller, P.J., Kroon, D., and Alexander, I., 1997. Monsoon-related variations in Zaire (Congo) sediment load and influence of fluvial silicate supply on marine productivity in the east equatorial Atlantic during the last 200,000 years. *Paleoceanography,* 12:463–481.

Schrader, H., and Sorknes, R., 1997. Peruvian coastal upwelling: late Quaternary productivity changes revealed by diatoms. *Mar. Geol.,* 144:117–130.

Schrader, H.-J., and Schuette, G., 1981. Marine diatoms. *In* Emiliani, C. (Ed.), *The Sea* (Vol. 7): New York (Wiley), 1179–1232.

Schuette, G., and Schrader, H., 1979. Diatom taphocoenosis in the coastal swelling area off western South America. *Nova Hedwigia Beih.,* 64:359–378.

Seitzinger, S.P., and Sanders, R.W., 1999. Atmospheric inputs of dissolved organic nitrogen stimulate estuarine bacteria and phytoplankton. *Limnol. Oceanogr.* 3:721–730.

Shackleton, N.J., Backman, J., Zimmerman, H., Kent, D.V., Hall, M.A., Roberts, D.G., Schnitker, D., Baldauf, J.G., Desprairies, A., Homrighausen, R., Huddlestun, P., Keene, J.B., Kaltenback, A.J., Krumsiek, K.A.O., Morton, A.C., Murray, J.W., and Westberg-Smith, J., 1984. Oxygen isotope calibration of the onset of ice-rafting and history of glaciation in the North Atlantic region. *Nature,* 307:620–623.

Shackleton, H.J., Hall, M.A., and Pate, D., 1995. Pliocene stable isotope stratigraphy of Site 846. *In* Pisias, N.G., Mayer, L.A., Janecek, T.R., Palmer-Julson, A., and van Andel, T.H. (Eds.), *Proc. ODP, Sci. Results,* 138: College Station, TX (Ocean Drilling Program), 337–355.

Shipboard Scientific Party, 1998a. Introduction: background, scientific objectives, and principal results for Leg 175 (Benguela Current and Angola-Benguela upwelling systems). *In* Wefer, G., Berger, W.H., and Richter, C., et al., *Proc. ODP, Init. Repts.,* 175: College Station, TX (Ocean Drilling Program), 7–25.

————, 1998b. Site 1083. *In* Wefer, G., Berger, W.H., and Richter, C., et al., *Proc. ODP, Init. Repts.,* 175: College Station, TX (Ocean Drilling Program), 313–337.

Sigman, D.M., Altabet, M.A., Francoise, R., and Whelan, J., 1997. Diatom microfossil N isotopes support the hypothesis of higher nitrate utilization in the Southern Ocean during the last ice age. *Pap. Amer. Chem. Soc.,* 1:69-GEOC (Abstract).

Tiedemann, R., Sarnthein, M., and Shackleton, N.J., 1994. Astronomic timescale for the Pliocene Atlantic $\delta^{18}O$ and dust flux records of Ocean Drilling Program Site 659. *Paleoceanography,* 9:619–638.

Treppke, U.F., Lange, C.B., Donner, B., Fischer, G., Ruhland, G., and Wefer, G., 1996. Diatom and silicoflagellate fluxes at the Walvis Ridge: an environment influenced by coastal upwelling in the Benguela system. *J. Mar. Res.,* 54:991–1016.

APPENDIX

Calculation for Diatom Accumulation Rate

Diatom Accumulation Rate (valves/cm² per k.y.) (e.g. Battarbee, 1986; Schuette and Schrader, 1979):

$$DAR = DMAR \cdot C_{dw}$$

Where:

DMAR = Dry Mass Accumulation Rate (g/cm per k.y.)

C_{dw} = diatom concentration per gram dry weight (valves/g)

Dry Mass Accumulation Rate (e.g. Battarbee, 1986; Schuette and Schrader, 1979):

$$DMAR = SR \cdot DBD_{sc}$$

Where:

SR = Sedimentation Rate (cm/k.y.) (NB must be calculated for each core section to avoid problems associated with postdrill handling)

DBD_{sc} = Salt Corrected Dry Bulk Density (g/cm³)

Concentration per gram dry weight (valves/g) (Battarbee and Kneen, 1982; Schuette and Schrader, 1979):

$$C_{dw} = C_d/W$$

Where:

C_d = diatom concentration (number of valves)

W = dry weight processed (g)

Diatom Concentration (by microsphere method) (Battarbee and Kneen, 1982):

$$C_d = (Y_{mi} \cdot X_d)/Y_{mc}$$

Where:

Y_{mi} = number of microspheres introduced

X_d = number of diatom valves counted

Y_{mc} = number of microspheres counted

Figure F1. Location of Site 1083, Leg 175 (20°53′S, 11°13′E; water depth = 2178 m; penetration = 201.3 mbsf). Major water masses over the site are shown in both aerial and schematic view along transect AB (modified from Berger et al., 1998; Dowsett and Willard, 1996; Hay and Brock, 1992), where a = Angola Current, b = Benguela Oceanic Current, c = poleward-flowing undercurrent, d = Benguela Coastal Current, and e = divergence and upwelling over shelf break.

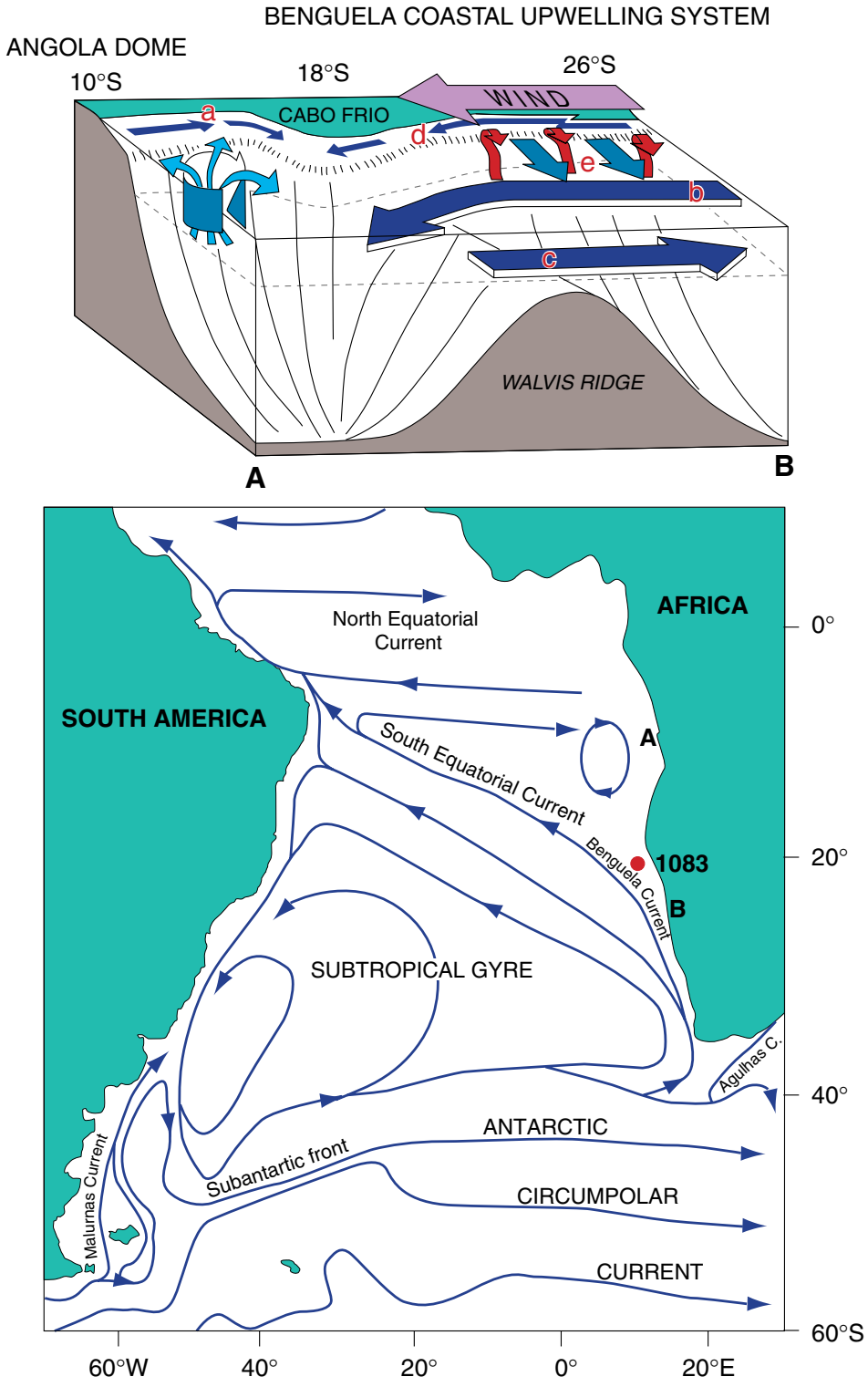

Figure F2. Downcore reconstructions vs. age for $\delta^{18}O$ vs. PDB (providing age model) after Vidal et al. (submitted, this volume [N2]); total organic carbon (TOC) (mass accumulation rate [MAR] is in grams per centimeter per thousand years); *Chaetoceros* resting spores (RS) (diatom accumulation rate [DAR] is in valves per square centimeters per thousand years); Southern Ocean diatoms (diatom accumulation rate); an $\delta^{15}N$ vs. air, where asterisks illustrate times of possible denitrification. "Hard" isothermal remanent magnetism curve (HIRM) shown for comparison. White/gray bands show interglacials/glacials, respectively. * = after Vidal et al. (submitted, this volume [N2]).

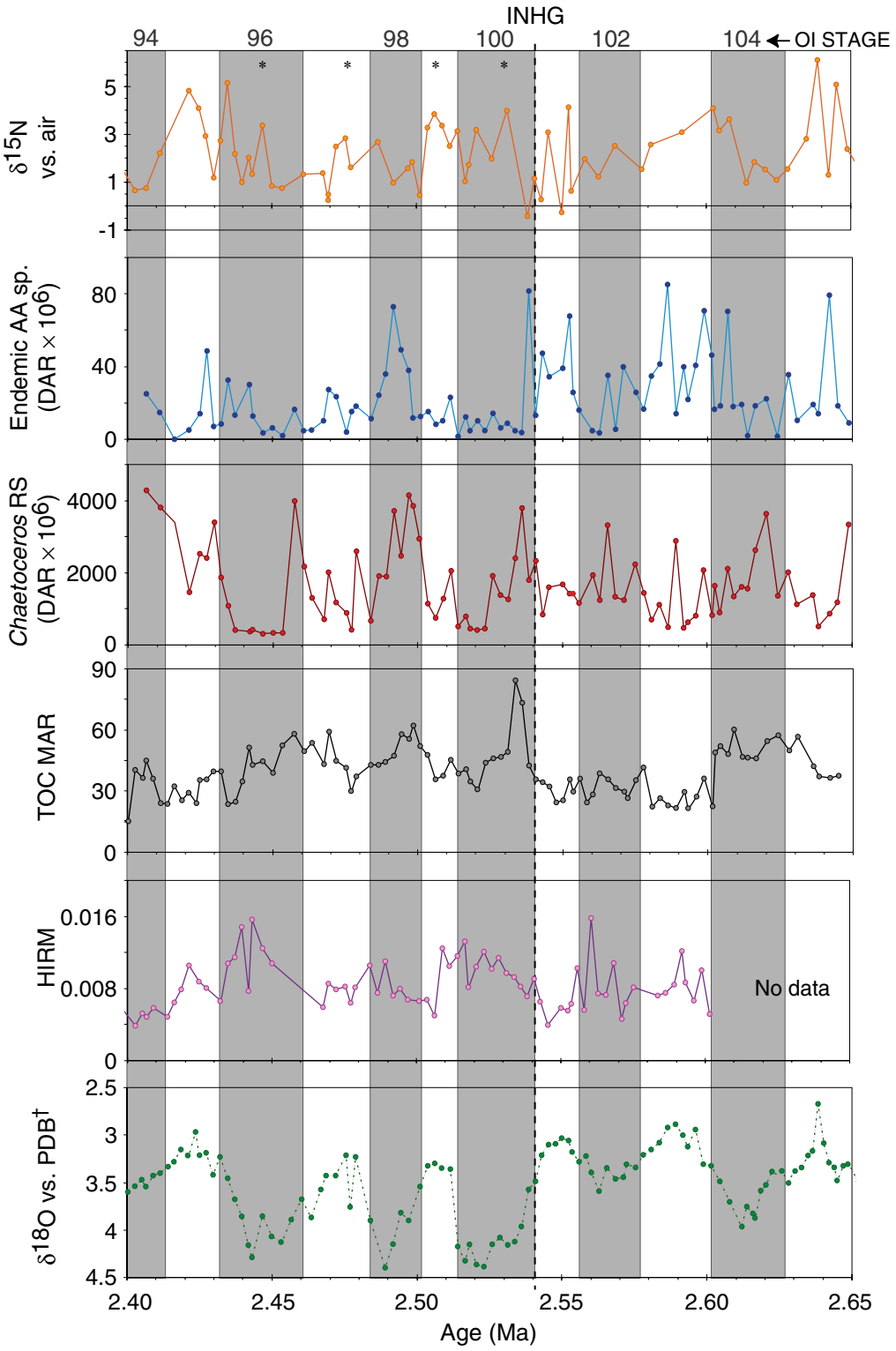

Figure F3. Simplified summary of events prior to and succeeding the intensification of the Northern Hemisphere glaciation (~2.54 Ma). General trends are noted directly from the data and show (**A**) wind-strength, (**B**) productivity, derived mainly from the *Chaetoceros* resting spore record, and (**C**) nutrient availability, where the direction of the arrow indicates the trend in the data.

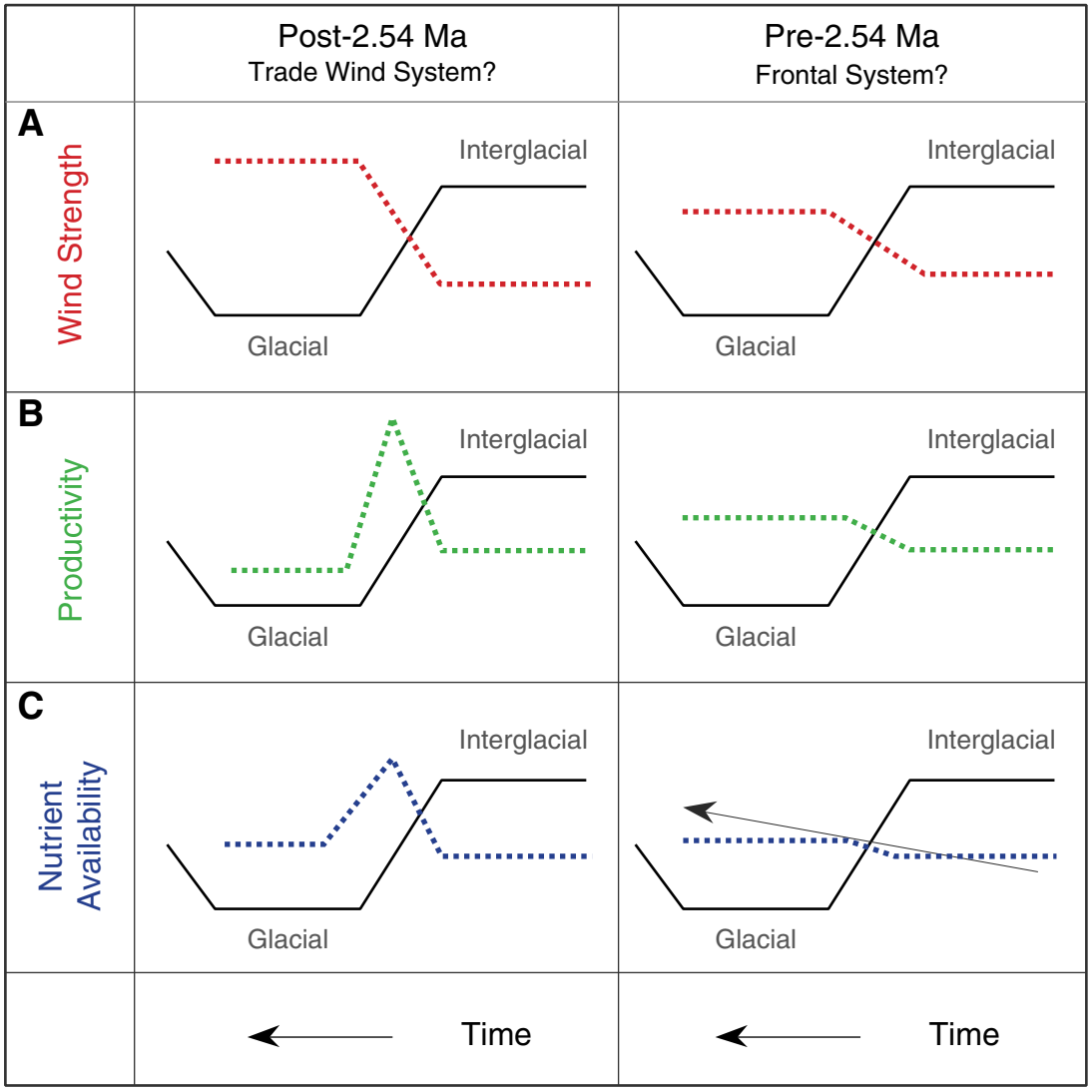

Table T1. Potential sources of alteration in the $\delta^{15}N$ signal.

Cause	Process	Effect	Examples of references
Denitrification	^{14}N returned to the atmosphere by denitrifying bacteria.	More ^{15}N enters marine NO_3^- pool, thereby limiting supply for phytoplankton.	Holmes et al. (1998; 1997; 1996); Naqvi et al. (1998); Pride et al. (1999); Francoise et al. (1993)
Nitrogen fixation	Cyanobacteria incorporate "new" nitrogen into system, for example.	More^{14}N enters marine NO_3^- pool, thereby increasing the amount of utilizable NO_3^-.	Altabet and Francoise (1994); Peters et al. (1978); Karl et al. (1997); Falkowski (1997)
Atmospheric input	Rain incorporates more "new" nitrogen into system.	More ^{14}N enters marine NO_3^- pool, thereby increasing the amount of utilizable NO_3^-.	Seitzinger and Sanders (1999); Capone and Carpenter (1982)
Terrigeneous input	By rivers, for example.	Marine NO_3^- pool becomes depleted/enriched depending upon contaminant source.	Holmes et al. (1998; 1997; 1996); Peters et al. (1978); Capone and Carpenter (1982); Falkowski (1997)
Grazing and recycling	Enrichment in ^{15}N at each trophic level.	More ^{15}N enters marine NO_3^- pool, thereby limiting supply for phytoplankton.	Bronk and Ward (1999); Altabet et al. (1991)
Diagenetic alteration	May occur both pre- and postburial. Preferential removal of ^{14}N during oxidative degradation of organic matter; however, evidence has been found indicating depletion of ^{15}N.	Will cause enrichment/depletion of ^{15}N in both the NO_3^- in the nitrate pool and in the sedimentary record.	Holmes et al. (1998; 1996); Altabet and Francoise (1994); Altabet et al. (1991); Sigman et al. (1997); Farrell et al. (1995)

CHAPTER NOTES*

N1. 12 February 2002—Rosell-Melé et al. was not published in this volume.

N2. 12 February 2002—Vidal et al. was not published in this volume.

*Dates reflect file corrections or revisions.